

Supplementary information

Validation procedure of the fit describing the increase of the interclonic intervals at the end of a seizure.

Our model predicts that interclonic intervals increase in an exponential manner at the end of a seizure. To validate this prediction in our clinical sample, we compare the exponential ($\log(\text{ICI}) \sim t$), logarithmic ($\text{ICI} \sim \log(t)$) and power law ($\log(\text{ICI}) \sim \log(t)$) fits. The results are shown in figure S1, S2 and S3.

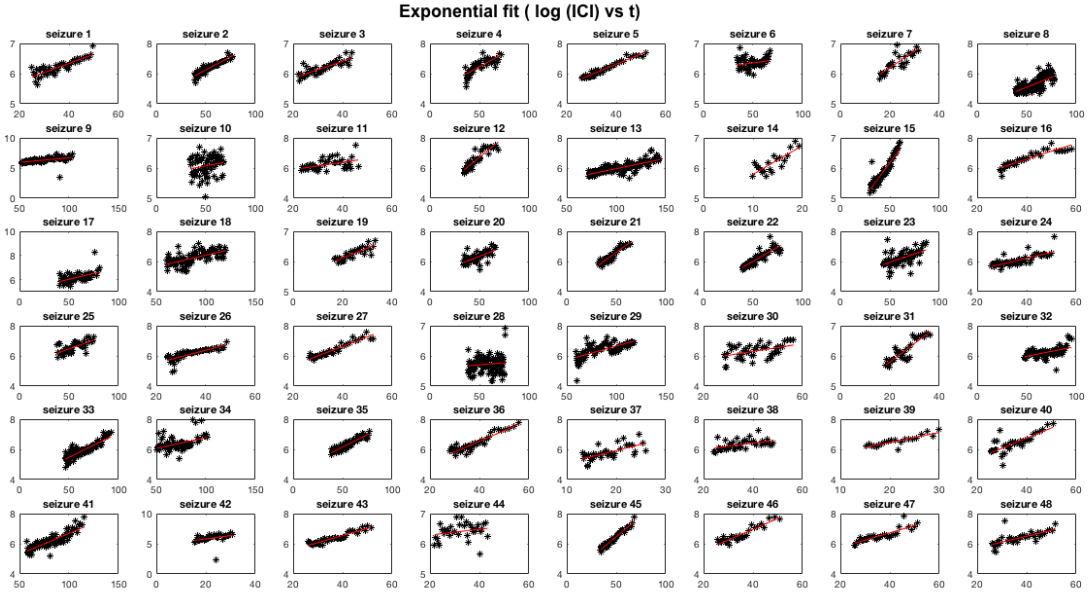


Figure S1 Exponential fit on our human EEG data set. Every panel represents one seizure from one individual. The black dots are the manually scored interclonic intervals (ICI), the red line represents the fit: $\log(\text{ICI}) = at + b$ [equivalent to the exponential relationship: $\text{ICI} = \exp(at+b)$] - the fit used in our model. On the vertical axis the Log(ICI) is shown, on the horizontal axis the time since the start of the clonic phase in seconds.

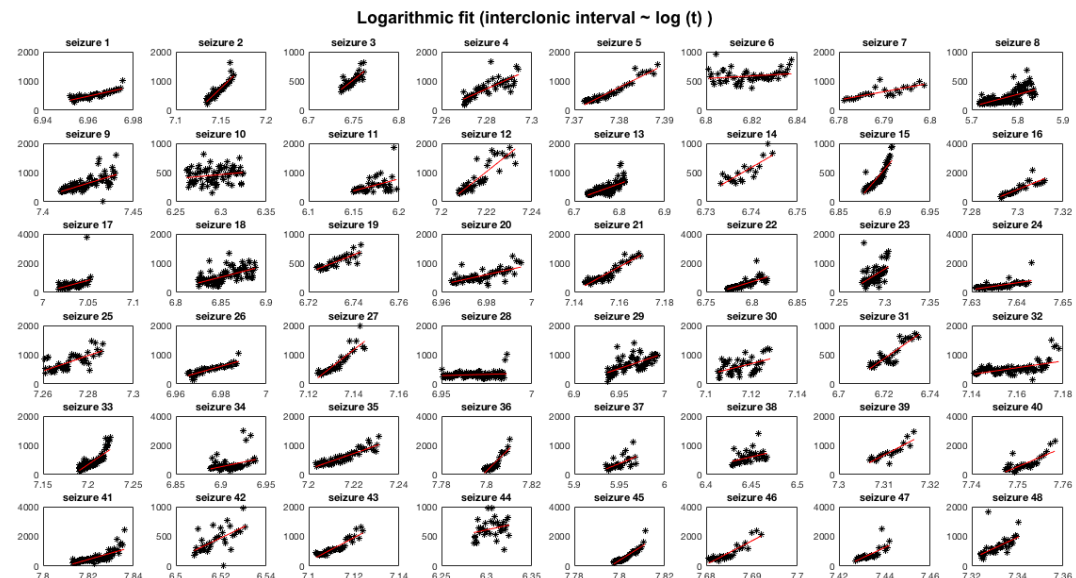


Figure S2 Logarithmic fit on our human EEG data set. Every panel represents one seizure from one individual. The black dots are the manually scored interclonic intervals (ICI), the red line represents

the fit: $ICI = a * \log(t) + b$, the fit in the model of Jirsa et al. On the vertical axis the ICI is shown in milliseconds, on the horizontal axis the $\log(\text{time})$ since the start of the clonic phase in seconds.

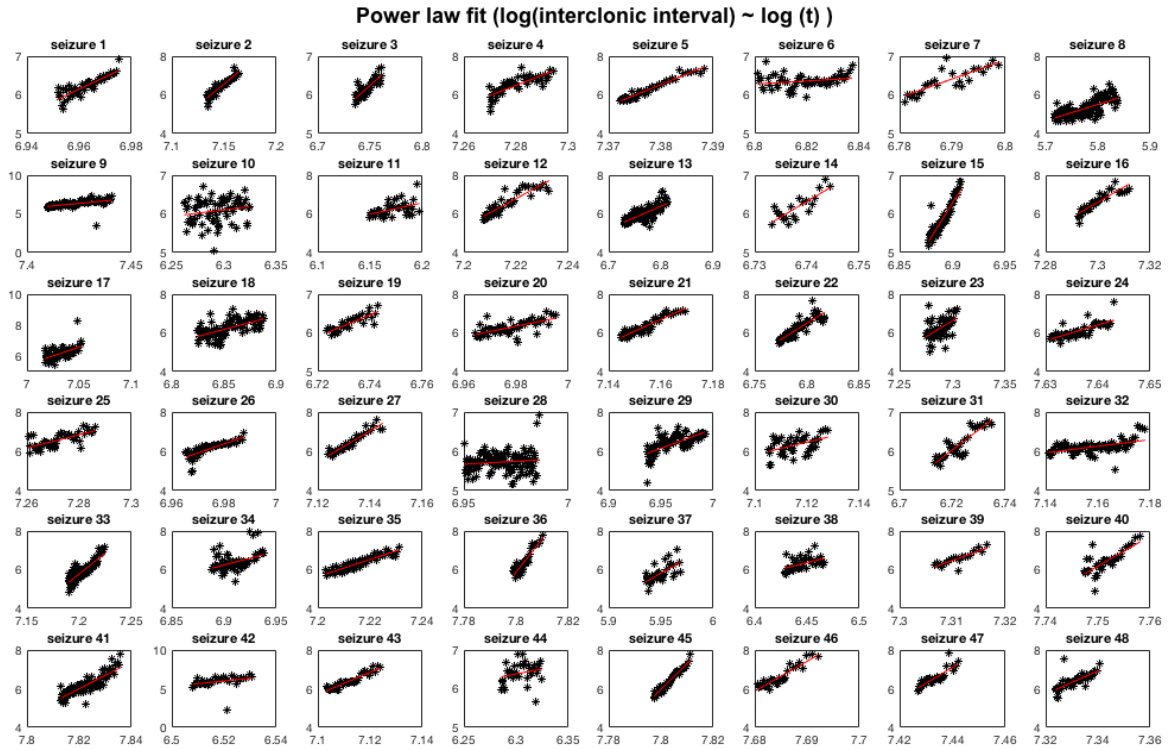


Figure S3 Power law fit on our human EEG data set. Every panel represents one seizure from one individual. The black dots are the manually scored interclonic intervals (ICI), the red line represents the fit: $\log(ICI) = a * \log(t) + b$, on the vertical axis $\log(ICI)$ is shown, on the horizontal axis the $\log(\text{time})$ since the start of the clonic phase in seconds.

The goodness of fit was calculated for each fit using R^2 , Root Mean Square Error (RMSE) and the relative systematic error defined as:

$$RM = \text{mean}(|\text{Obs}-\text{fit}|)/(\text{Obs})$$

where $|x|$ denotes the absolute value of x .

This latter calculation, in our view, better takes into account the error of the fit when the interclonic interval is small.

A R^2 value close to 1 denotes a good fit. The lower the RMSE and relative systematic error value the better fit. The results of the R^2 , RMSE and RM are shown in table S1. There was no significant difference between the R^2 and RMSE of the fits.

The RM, however, was significantly larger in the logarithmic fit compared to the exponential fit ($p < 0.0001$), see figure S4. The RM of the exponential and power law fits did not significantly differ, see figure S5.

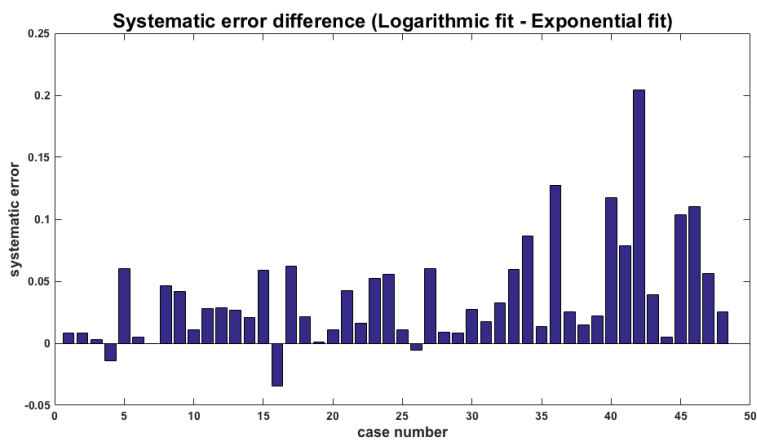


Figure S4 Histogram showing the difference in relative systematic error (RM) between the logarithmic fit and the exponential fit for each seizure. The seizures 1-48 are shown on the horizontal axes, the systematic error is shown on the vertical axis. For 45 of the 48 seizures, the logarithmic fit (figure S2) has a greater systematic error than the exponential fit (figure S1).

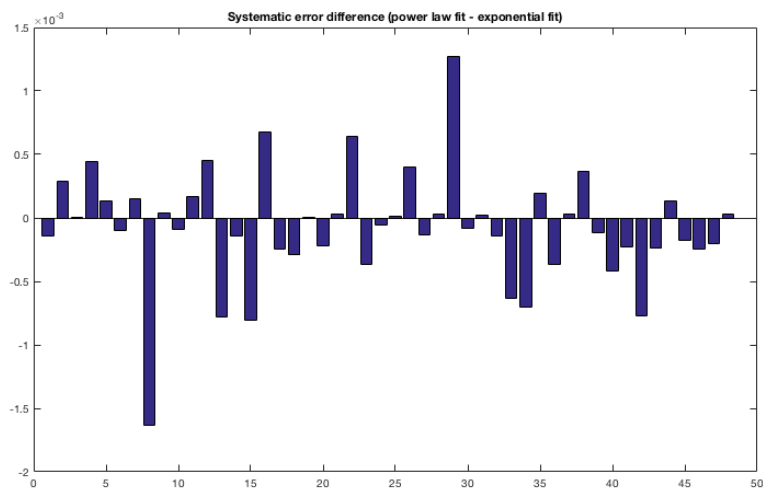


Figure S5 Histogram showing the difference in relative systematic error (RM) between the power law fit and the exponential fit for each seizure. The seizures 1-48 are shown on the horizontal axes, the systematic error is shown on the vertical axis. There was no statistically significant difference between the systematic error of the power law fit (figure S3) and the systematic error of the exponential fit (figure S1).

Table S1: Errors of the exponential, logarithmic and power law fit.

For each case (1-48) and fit (exponential, logarithmic, power law), the error measures are given. Exp=exponential, log=logarithmic, powerL=power law, $R^2=R^2$, RM=relative systematic error, RMSE=root-mean square error.

Case	R ² exp	R ² log	R ² powerL	RM exp	RM log	RM powerL	RMSE exp	RMSE log	RMSE powerL
1	0.779	0.744	0.780	0.092	0.100	0.091	62.23	66.94	62.06
2	0.870	0.856	0.869	0.101	0.108	0.101	98.75	103.81	98.90
3	0.683	0.668	0.683	0.089	0.091	0.089	62.09	63.57	62.03
4	0.564	0.634	0.563	0.225	0.212	0.226	211.12	193.54	211.45
5	0.926	0.923	0.925	0.085	0.143	0.085	98.30	99.73	98.89
6	0.043	0.046	0.044	0.126	0.131	0.126	102.42	102.24	102.36
7	0.599	0.621	0.598	0.122	0.122	0.122	122.65	119.12	122.73
8	0.485	0.479	0.490	0.211	0.251	0.209	70.67	71.12	70.33
9	0.426	0.457	0.426	0.408	0.449	0.408	188.64	183.36	188.58
10	0.019	0.040	0.019	0.258	0.269	0.258	128.84	127.45	128.84
11	0.163	0.190	0.163	0.231	0.258	0.231	240.03	236.13	240.02
12	0.682	0.792	0.679	0.183	0.210	0.183	279.45	226.13	280.87
13	0.620	0.594	0.625	0.126	0.150	0.125	102.51	106.02	101.91
14	0.707	0.661	0.708	0.158	0.179	0.158	97.74	105.13	97.61
15	0.885	0.803	0.887	0.093	0.149	0.092	57.70	75.46	57.10
16	0.664	0.777	0.662	0.166	0.132	0.167	241.53	196.75	242.32
17	0.142	0.155	0.143	0.193	0.254	0.193	372.17	369.28	371.95
18	0.366	0.383	0.365	0.257	0.278	0.257	183.46	180.95	183.60
19	0.693	0.692	0.693	0.086	0.087	0.086	58.73	58.88	58.74
20	0.503	0.483	0.505	0.193	0.204	0.193	150.11	153.18	149.88
21	0.899	0.883	0.899	0.110	0.150	0.110	98.15	106.07	98.48
22	0.570	0.615	0.567	0.133	0.146	0.133	200.95	190.11	201.65
23	0.315	0.298	0.316	0.263	0.315	0.263	238.09	240.94	237.81
24	0.420	0.399	0.420	0.140	0.195	0.140	195.42	198.79	195.30
25	0.532	0.518	0.533	0.187	0.198	0.187	183.97	186.80	183.86
26	0.768	0.778	0.768	0.162	0.156	0.162	77.75	76.06	77.82
27	0.825	0.819	0.824	0.102	0.161	0.102	159.92	162.57	160.34
28	0.013	0.031	0.013	0.186	0.195	0.186	98.93	98.01	98.93
29	0.376	0.453	0.373	0.269	0.279	0.270	205.00	192.02	205.48
30	0.234	0.241	0.234	0.356	0.383	0.356	227.70	226.62	227.56
31	0.808	0.793	0.808	0.123	0.140	0.123	83.25	86.52	83.28
32	0.321	0.322	0.324	0.195	0.227	0.195	168.56	168.48	168.19
33	0.792	0.702	0.795	0.170	0.227	0.169	104.50	125.10	103.70
34	0.122	0.146	0.124	0.249	0.334	0.248	425.37	419.59	424.96
35	0.853	0.843	0.853	0.112	0.124	0.113	89.34	92.41	89.46
36	0.921	0.832	0.921	0.159	0.285	0.159	139.76	203.52	139.35
37	0.347	0.370	0.346	0.263	0.288	0.263	159.81	156.93	159.87
38	0.149	0.175	0.148	0.205	0.221	0.206	184.45	181.60	184.58
39	0.793	0.749	0.793	0.123	0.145	0.123	122.17	134.48	122.00
40	0.711	0.603	0.712	0.270	0.386	0.269	259.61	304.36	259.07

41	0.699	0.618	0.701	0.182	0.259	0.181	184.17	207.44	183.46
42	0.309	0.394	0.310	1.342	1.545	1.341	159.13	149.02	159.08
43	0.890	0.845	0.891	0.092	0.130	0.092	83.79	99.64	83.55
44	0.043	0.062	0.043	0.202	0.208	0.203	151.59	150.10	151.66
45	0.930	0.841	0.931	0.083	0.185	0.083	104.04	156.96	103.54
46	0.874	0.808	0.874	0.162	0.270	0.161	196.51	242.05	196.29
47	0.581	0.559	0.582	0.133	0.188	0.133	263.32	270.34	263.20
48	0.351	0.341	0.351	0.160	0.185	0.160	241.53	243.35	241.47